Effect of Ti seed layer on the magnetization reversal process of Co/NiFe/Al-oxide/NiFe junction films

doi: 10.1063/1.1459598

Effect of Ti seed layer on the magnetization reversal process of Co/NiFe/Al-oxide/NiFe junction films

Andrew C. C. Yu[a)]
Department of Materials Solution Development, Sony Corp., 3-4-1 Sakuragi, Tagajo, Miyagi 985-0842, Japan

Amanda K. Petford-Long
Department of Materials, University of Oxford, Parks Road, Oxford OX1 3PH, United Kingdom

Kevin O'Grady
Department of Physics, University of York, Heslington, York Y010 5DD, United Kingdom

Terunobu Miyazaki
Department of Applied Physics, Graduate School of Engineering, Tohoku University, Sendai 980-8579, Japan

(Received 31 July 2001; accepted for publication 17 January 2002)

Ti/Co/NiFe/Al-oxide/NiFe (F1) and Co/NiFe/Al-oxide/NiFe (F2) junction films were characterized using high-resolution electron microscopy (HREM), Lorentz transmission electron microscopy (LTEM), and alternating gradient force magnetometry (AGFM). HREM images showed that the Ti seed layer induced a strong ⟨111⟩ texture in the bottom Co/NiFe bilayer. The ferromagnet/Al-oxide interfaces in F1 showed correlated waviness, while the interface waviness in F2 appeared uncorrelated. Thus, ''orange-peel'' coupling effect was more significant in F1 than in F2, which was confirmed by the steep slope of the magnetization curve in the ''antiparallel'' magnetization configuration for F1. The LTEM *in situ* magnetizing experiment results and the AGFM measurement of magnetization curves showed that both junction films possessed a two-stage magnetization reversal characteristic—magnetization of the top NiFe layer reversed first followed by the reversal of the bottom Co/NiFe bilayer. LTEM observation revealed that the magnetization reversal of the top NiFe layer was via domain wall motion, while the reversal of the bottom Co/NiFe bilayers was mainly by wall motion together with a small degree of moment rotation. Domain wall mobility in the Co/NiFe bilayer of F1 was higher due to the strong crystallographic texture and large grain size appeared in the bilayer. © *2002 American Institute of Physics.*
[DOI: 10.1063/1.1459598]

I. INTRODUCTION

It has been reported that the microstructure of ferromagnet/insulator/ferromagnet type magnetic tunnel junctions can highly affect the magnetization process and the two-stage magnetization reversal characteristic of the junctions.[1] Also, many research groups have discussed that various seed layer materials can induce a strong ⟨111⟩ texture on the adjacent layer,[2,3] for example a Ti seed layer has been shown to enhance the structural quality of Co/Cu/Co/MnFe films giving a strong ⟨111⟩ texture and large grain size.[4] The intent of this article is to study the effect of the Ti seed layer on the microstructure and thus on the magnetization reversal process of Co/NiFe/Al-oxide/NiFe junction.

Lorentz transmission electron microscopy (LTEM) is a very useful characterization technique to examine the submicron scale magnetic features of a wide range of magnetic thin film materials.[5] In LTEM, the Fresnel mode and Foucault mode are two common configurations used to image the magnetic domain structure. For the Fresnel mode, with the objective lens defocused, the effect of the Lorentz deflections becomes apparent, therefore domain walls appear as bright and dark lines. For the Foucault mode, the objective aperture is displaced from its central position until it intercepts electrons which have passed through one set of domains magnetized in the same direction, while transmitting electrons which have passed through another set of domains magnetized in a different direction. Domains in the former set appear darker than domains in the latter set. The spatial resolution of Foucault images is better than that of Fresnel images because the former are in focus; however, Foucault images are more difficult to obtain than Fresnel images. Magnetization reversal process of magnetic thin films can also be observed *in situ* using LTEM with a magnetizing stage mounted on the sample holder. We aim at observing the magnetization process and the reversal mechanism of Ti/Co/NiFe/Al-oxide/NiFe and Co/NiFe/Al-oxide/NiFe junction films directly by conducting *in situ* magnetizing experiments. Thus, the effect of the Ti seed layer on the magnetization reversal process of the junction film can be investigated. Meanwhile, the microstructure of the junctions films were characterized using high-resolution electron microscopy (HREM), therefore a better understanding of the correlation

[a)]Author to whom all correspondence should be addressed; electronic mail: andrew.yu@jp.sony.com

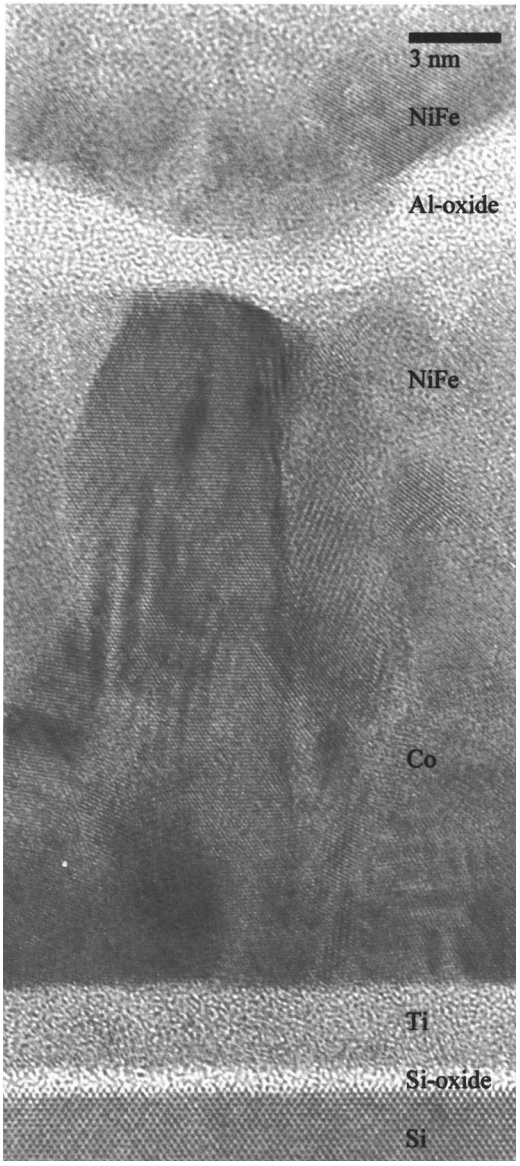

FIG. 1. HREM image of a cross section of Ti/Co/NiFe/Al-oxide/NiFe film (F1).

between the microstructure and the reversal mechanism of the junction films can be obtained. Furthermore, magnetization curves, which can provide useful macroscopic magnetization reversal information, for the junctions films are presented.

II. EXPERIMENTAL DETAILS

The junction films were fabricated using magnetron sputtering. The Ti, NiFe (note: the atomic weight ratio of the NiFe reported in this article is $Ni_{80}Fe_{20}$), and Co layers were dc sputtered, while the Al-oxide layer was prepared by oxidizing a rf sputtered Al layer in air for about 72 h before deposition of the top NiFe layer. The base pressure of the vacuum chamber was about 3×10^{-6} mbar, and the Ar pressure used for sputtering was about 6×10^{-3} mbar. The junction films were deposited on carbon coated Cu grids and in-plane images were observed in a JEOL 4000EX transmission electron microscope fitted with a JEOL AMG40 low-

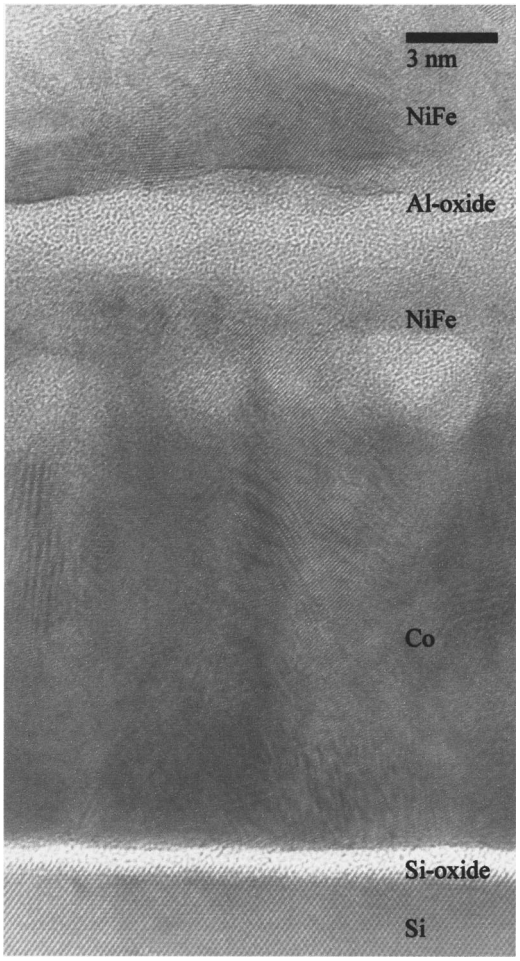

FIG. 2. HREM image of a cross section of Co/NiFe/Al-oxide/NiFe film (F2).

field objective lens pole piece. The incident electron beam energy was set at 400 keV. A spatial resolution of about 1 nm was achieved with a magnetic field at the specimen position of less than 1.3 Oe. *In situ* magnetizing experiments were carried out to study the magnetization reversal process of the Ti/Co/NiFe/Al-oxide/NiFe and Co/NiFe/Al-oxide/NiFe junction films during the magnetization cycle. The junction film specimens were placed in a specially designed side-entry specimen holder fitted with a pair of magnetizing coils which can produce a magnetizing field in the specimen plane. The field strength can be varied up to 400 Oe. The Fresnel mode was employed for the *in situ* magnetizing experiments because it can be more conveniently used to trace the domain activity in real time. Cross sections of the junction films were observed using HREM in a 400 keV JEOL 4000EX transmission electron microscope with a top-entry specimen holder. Alternating gradient force magnetometry (AGFM) was used to measure the magnetization curves of the junction films.

III. RESULTS AND DISCUSSION

A. Microstructure

Figures 1 and 2 show cross-sectional HREM images of the Ti/Co/NiFe/Al-oxide/NiFe (5/23/20/3/20 nm) (F1) and

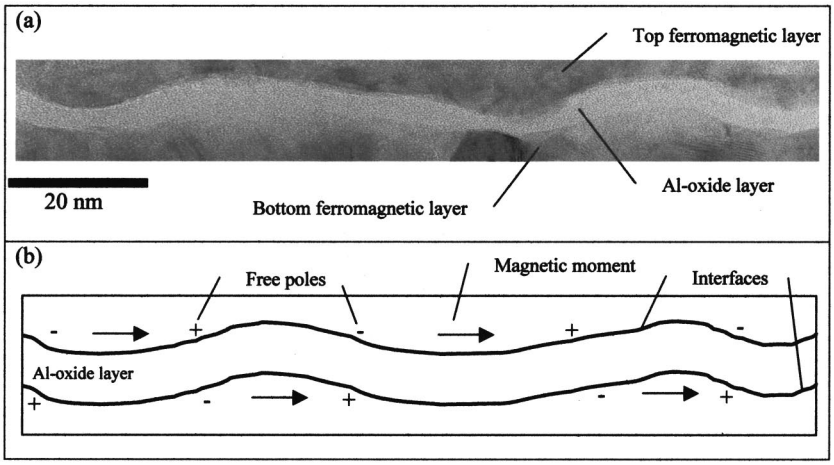

FIG. 3. Correlated waviness of the interfaces in F1 junction film. (a) Low magnification cross-sectional TEM image. (b) Schematic diagram of (a).

Co/NiFe/Al-oxide/NiFe (23/20/3/20 nm) (F2) junction films, respectively. In both junction films, the top NiFe layer and the bottom Co/NiFe bilayer were clearly separated by the Al-oxide layer. Most of the Al was oxidized after 72 h exposure in air. There was no polycrystalline Al observed and the Al-oxide layer appeared amorphous. In F1, the Co/NiFe bilayer, which was grown on top of the Ti seed layer, showed a strong ⟨111⟩ texture in the growth direction (Fig. 1). On the other hand, the Co/NiFe bilayer in F2, which was deposited on native amorphous Si-oxide, appeared polycrystalline and the grains were randomly oriented (Fig. 2). It is also observed that the strongly textured grains in the Co/NiFe bilayer in F1 were generally larger than the randomly oriented grains in bilayer in F2. The top NiFe layer in both F1 and F2 was polycrystalline with random grain orientation. The Ti seed layer had no direct effect on the crystallographic texture of the top NiFe layer in F1 because the Al-oxide layer separated it from the bottom enhanced texture Co/NiFe layer, therefore no enhanced texture was induced in the top NiFe layer.

Figures 3(a) and 4(a) are low magnification cross-sectional transmission electron microscopy (TEM) images showing longer section of the interfaces in F1 and F2, respectively. It can be observed that the interface between the Co/NiFe bilayer and the Al-oxide layer in F1 was wavier than that in F2. Such a wavy interface led to the formation of a wavy Al-oxide layer in F1, and consequently the Al-oxide layer/top NiFe layer interface as well as the top NiFe layer became wavy in F1. Furthermore, correlated waviness of the interfaces between the Al-oxide layer and the ferromagnetic layers in F1 was observed. On the other hand, the interfaces between the Al-oxide layer and the ferromagnetic layers in F2 showed uncorrelated waviness. The relatively flat NiFe/Al-oxide interface in F2 was possibly attributed to smaller grain size in the Co/NiFe bilayer. The correlated waviness of the interfaces in F1 is schematically shown in Fig. 3(b). Such correlated waviness of the interfaces may lead to a magnetostatic coupling effect called ''orange-peel'' coupling.[6] Néel explained that the orange-peel coupling effect is due to the free magnetic poles of opposite sign formed on the interfaces, which show correlated waviness.[7] As a result, the magnetic moments in the top NiFe layer and the bottom Co/NiFe bilayer were ferromagnetically coupled. In F2, the orange-peel coupling effect was expected lower than that in F1 because the interface waviness was uncorrelated [Fig. 4(b)], thus the formation of free magnetic poles was not promoted effectively, therefore the effect of free magnetic poles on ferromagnetic coupling between the top NiFe layer and the bottom Co/NiFe bilayer was weak. It has also been reported by some other researchers on an observation of correlated waviness of the interfaces in some spin-valve structure with a Ta seed layer, and hence, the effect of magnetostatic orange-peel coupling in the spin valve.[8]

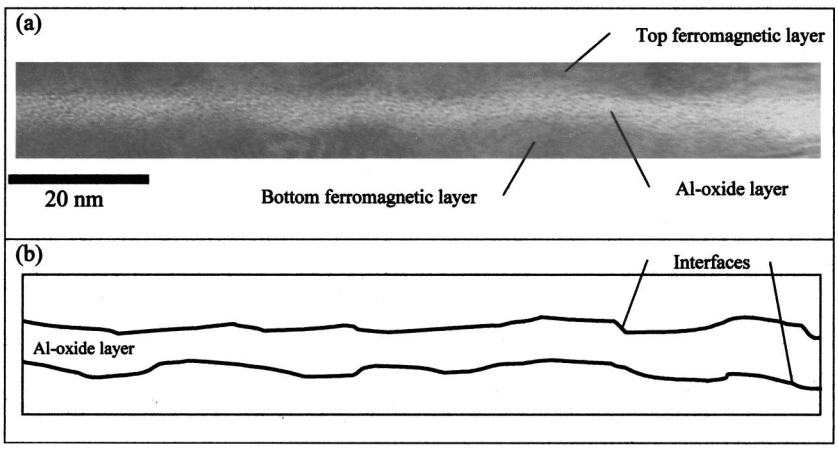

FIG. 4. Uncorrelated waviness of the interfaces in F2 junction film. (a) Low magnification cross-sectional TEM image. (b) Schematic diagram of (a).

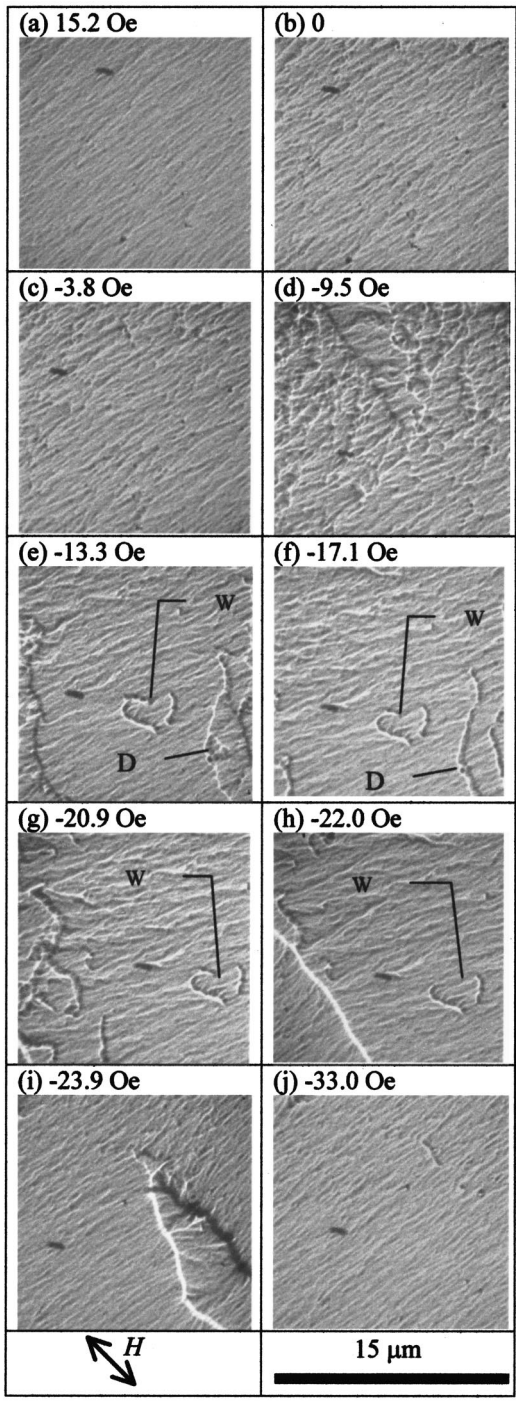

FIG. 5. LTEM Fresnel images of the magnetization process for F1. The direction of the applied field *H* and the field values in oersteds are shown; all images are of the same area. Magnetization reversal of the top NiFe layer occurred between (c) and (e). An antiparallel magnetization configuration existed between (e) and (h). Magnetization reversal of the bottom Co/NiFe bilayer began at (h) and ended before (j). A 360° wall (marked *W*) formed at (e), remained at (f) and (g), broke at (h), and disappeared at (i). A domain wall that was pinned by some defect is marked *D* in (e) and (f).

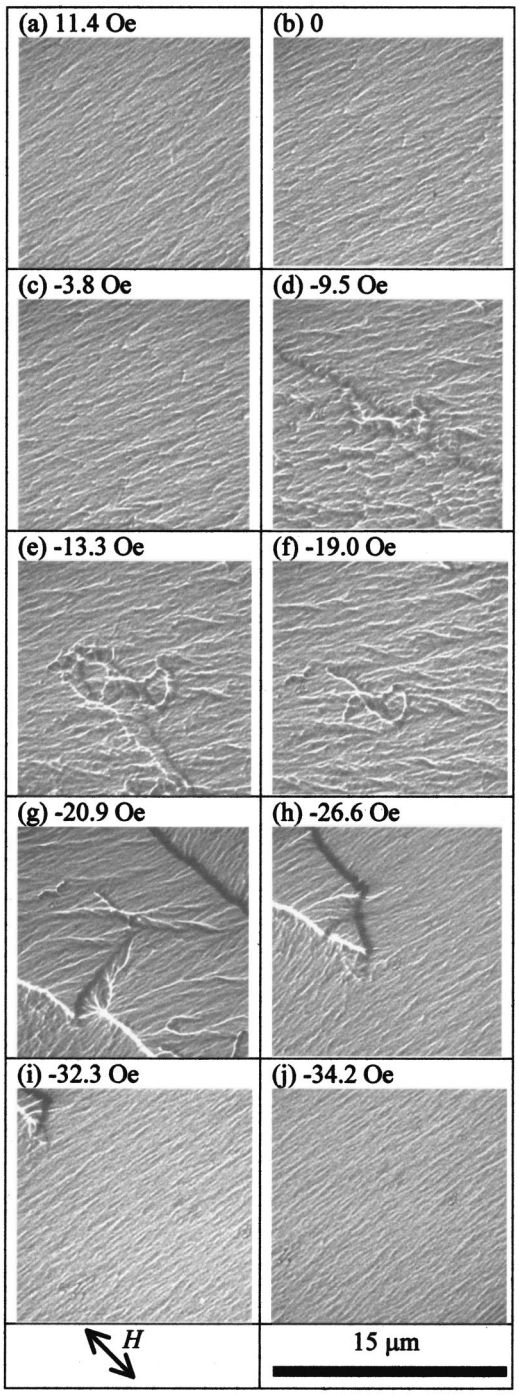

FIG. 6. LTEM Fresnel images of the magnetization process for F2. The direction of the applied field *H* and the field values in oersteds are shown; all images are of the same area. Magnetization reversal of the top NiFe layer occurred between (c) and (e). An antiparallel magnetization configuration existed between (e) and (g). Magnetization reversal of the bottom Co/NiFe bilayer began at (g) and ended before (j).

B. Lorentz transmission electron microscopy studies

A field of 400 Oe was applied to both F1 and F2 initially in order to saturate the top NiFe layer and the bottom Co/NiFe bilayer. The field was then reduced to zero [Figs. 5(b) and 6(b)], after that the field was increased in the reverse direction (negative field). The magnetization ripple contrast increased gradually [compare Figs. 5(a) and 6(a) in a positive field with Figs. 5(c) and 6(c) in a small negative field, respectively]. The ripple rotated very slightly in a small negative field in both F1 and F2, which indicated some moment rotation [Figs. 5(c) and 6(c)]. Increasing the field in the reverse direction led to magnetization reversal of the top NiFe layer between −3.8 and −13.3 Oe in both F1 [Figs. 5(c)–5(e)] and F2 [Figs. 6(c)–6(e)] mainly by domain wall mo-

tion. It is believed that the top NiFe layer is magnetically softer than the Co/NiFe bilayer, thus the magnetization of the top NiFe layer reversed before the magnetization reversal of the Co/NiFe bilayer occurred.

It was observed that the NiFe domain walls, which were not pinned by defects on the films, were moving rapidly as the applied field was increasing. The pinned NiFe domain walls [see, e.g., a pinned wall marked *D* in Figs. 5(e) and 5(f)] remained in the film until a higher field was applied. There was also a 360° wall loop structure [marked *W* in Figs. 5(e)–5(h)] observed in F1 (such loop structure will be discussed further later). The disappearance of the NiFe domain walls indicated that the magnetization reversal of the top NiFe layer was complete. The magnetization directions of the top NiFe layer and the Co/NiFe bilayer were generally antiparallel at this stage.

When the applied field was increased further, magnetization reversal of the Co/NiFe bilayer in F1 occurred between −20.9 and −33.0 Oe [Figs. 5(g)–5(j)]. The magnetization reversal of the Co/NiFe bilayer in F2 reversed between −20.9 and −34.2 Oe [Figs. 6(g)–6(j)]. The magnetization reversal of the Co/NiFe bilayer in both F1 and F2 was mainly via the motion of domain walls, which is the main reversal mechanism seen in NiFe because of its magnetic softness and low magnetic anisotropy, together with a small degree of moment rotation (by observing the rotation of the magnetization ripple). Observation of such Co/NiFe domain wall motion is similar to the reversal mechanism of the Co/NiFe bilayer, which is also mainly due to domain wall motion[1] with a small degree of moment rotation. The results of magnetization reversal mechanism of the Co/NiFe bilayer in F1 and F2 have provided further experimental evidence on the description that the magnetization reversal of ferromagnetic bilayer appears to be dominated by the layer closest to the Al-oxide layer.[9] Based on the LTEM results, the magnetization reversal of the Co/NiFe bilayer in F1 took a slightly shorter field range than that in F2. It was due to the generally larger grain size and the strong crystallographic texture of the bottom Co/NiFe bilayer induced by the Ti seed layer in F1, thus fewer grain boundaries existed for domain wall pinning, therefore domain wall mobility was slightly higher in the Co/NiFe bilayer in F1. After the magnetization reversal of Co/NiFe bilayer, the magnetization directions of the NiFe layer and the bilayer were parallel and aligned in the reverse field direction, and only magnetization ripple was observed [Figs. 5(j) and 6(j)].

The domain walls in the bottom Co/NiFe bilayer show stronger contrast and were relatively wider in the LTEM images than those in the top NiFe layer because the bottom Co/NiFe bilayer was thicker and magnetically stronger than the top NiFe layer [compare Figs. 5(d) and 5(h) or Figs. 6(d) and 6(h)]. The magnetic contrast marked *W* in Fig. 5 was a 360° wall loop structure.[10] The 360° wall loop formed as the applied field decreased to zero from saturation and increased in the reverse direction at −13.3 Oe [Fig. 5(e)]. As the reverse field increased, most of the domain walls moved except the 360° wall loop [Fig. 5(f)]. The 360° wall loop remained throughout the magnetization reversal process of the top NiFe layer [Figs. 5(e)–5(g)], and it started breaking at

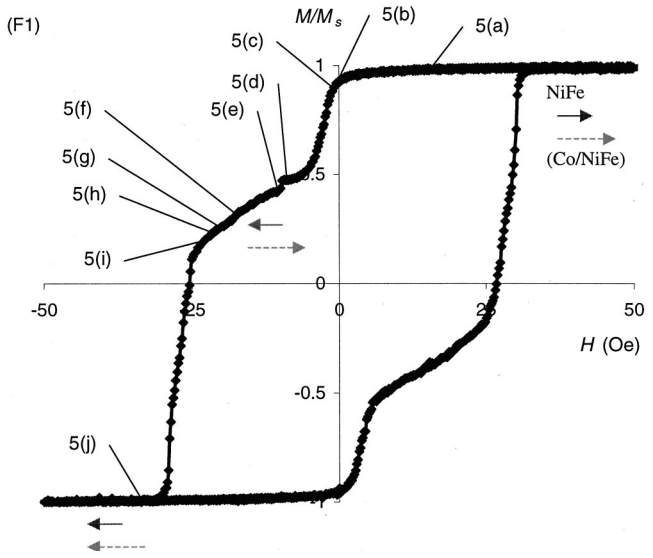

FIG. 7. Normalized magnetization vs applied field for F1. Corresponding domain structure at different field values along the magnetization curve is shown in Fig. 5.

−22.0 Oe during the magnetization reversal of the bottom Co/NiFe layer [Fig. 5(h)]. Finally, the 360° wall loop disappeared at −23.9 Oe [Fig. 5(i)]. The diameter of the 360° wall loop was about 4 μm. The magnetization directions inside and outside the loop at a nonzero field were parallel while the magnetization orientations near and at the wall were very complex. A number of research groups have reported the observation of, and explained the formation of, such 360° wall loop structures in different magnetic layered films.[11,12] The existence of such loop structure in single isolated Permalloy films has been known for some time and they are usually associated with a clearly visible pinning point such as an inclusion.[13] The 360° wall loop structures can also exist despite an absence of obvious topological pinning sites in some magnetic layered systems. Repetition of the magnetization cycle showed that there was a strong tendency for rather similar complex domain structures to form in approximately the same places within the sample, which suggests that there were locations where 360° wall loop structures were significantly stabilized. The high fields required for the wall loop annihilation provide further evidence for this observation.[14]

C. Alternating gradient force magnetometry measurements

Magnetization curves for F1 and F2 junction films are shown in Figs. 7 and 8, respectively. The magnetic field was applied in-plane for the AGFM measurement. Corresponding domain structure images at different field values along the magnetization curve are shown in Fig. 5 (for F1) and Fig. 6 (for F2) [e.g., 5(a) marked in Fig. 7 corresponds to image (a) in Fig. 5]. Two-stage magnetization reversals are clearly shown in both Figs. 7 and 8. As the total saturation magnetization of the top NiFe layer was smaller than that of the Co/NiFe bilayer, therefore the (first) smaller drops of the magnetization curves from saturation was corresponding to

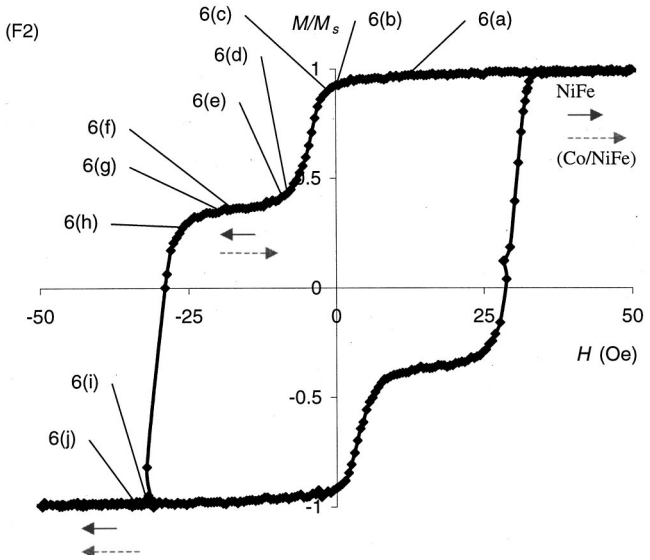

FIG. 8. Normalized magnetization vs applied field for F2. Corresponding domain structure at different field values along the magnetization curve is shown in Fig. 6.

the reversal of the top NiFe layer, while the (second) larger drop of the magnetization curve was contributed by the reversal of the Co/NiFe bilayer. It can then be shown that the magnetization reversal of the top NiFe layer occurred between 5(c) and 5(e) in F1 (Fig. 7), and between 6(c) and 6(e) in F2 (Fig. 8).

The antiparallel magnetization configuration exists between 5(e) and 5(g) in F1 (Fig. 7), and between 6(e) and 6(g) in F2 (Fig. 8). The nonzero slope between 5(e) and 5(h) in F1 indicated that the angle between the top NiFe layer and the bottom Co/NiFe bilayer was not exactly equal to 180° but it was decreasing in the antiparallel magnetization configuration region. Furthermore, the relatively steep slope between 5(e) and 5(g) in Fig. 7 was due to magnetostatic orange-peel coupling between the top NiFe layer and the bottom Co/NiFe bilayer in F1, which was resulting from the correlated waviness of the interfaces in F1. Thus, the Co/NiFe bilayer magnetization was induced to reverse after the top NiFe layer magnetization reversed to the applied field direction. On the other hand, the slope between 6(e) and 6(g) in F2 was relatively flat, which implied that the effect of magnetostatic orange-peel coupling was relatively weak in F2 because the interfaces showed uncorrelated waviness.

The observation of a single ''second drop'' of the normalized magnetization curve, which corresponded to the most rapid part of the magnetization reversal of the bottom Co/NiFe bilayer, and the change of normalized magnetization value for that reversal process, confirmed that the magnetization of the Co and the NiFe in the Co/NiFe bilayer of F1 and F2 were ferromagnetically coupled to each other. Thus, the magnetization reversal of the Co/NiFe bilayer began at 5(g) and ended before 5(j) in F1 (Fig. 7), and it began at 6(g) and ended before 6(j) in F2 (Fig. 8). The magnetostatic orange-peel coupling effect could also be a cause of the shorter reversal field range for the Co/NiFe bilayer in F1 (compared with the reversal field range for the Co/NiFe bilayer in F2) as the Co/NiFe bilayer could be induced to switch by the top NiFe layer. The magnetization of the top NiFe layer and the bottom Co/NiFe bilayer are parallel to the reverse field direction after 5(j) in F1 (Fig. 7) and 6(j) in F2 (Fig. 8). The magnetization curves measured using AGFM were consistent with the LTEM *in situ* magnetizing examinations for both F1 and F2 junction films.

IV. CONCLUSIONS

Both Ti/Co/NiFe/Al-oxide/NiFe (F1) and Co/NiFe/Al-oxide/NiFe (F2) junction films showed a characteristic two-stage magnetization process with the first magnetization reversal occurred at the top NiFe layer followed by the second reversal existed at the bottom Co/NiFe bilayer. The slope of the magnetization curve for F1 in the antiparallel magnetization configuration region was much steeper than that for F2 indicating that significant orange-peel coupling effect, which was due to correlated ferromagnet/Al-oxide interface waviness, existed in F1. LTEM observation showed that magnetization reversal of the top NiFe layer and the bottom Co/NiFe bilayers was mainly via domain wall motion. The strong crystallographic texture and large grain size appeared in the Co/NiFe bilayer of F1 induced higher domain wall mobility. In order to avoid the appearance of correlated waviness in samples with seed layers, adjustment of sputtering conditions and/or alternation of the bottom ferromagnetic layer structure are possible solutions.

ACKNOWLEDGMENTS

A. C. C. Y. would like to thank R. C. Doole at the University of Oxford for technical assistance in electron microscopy and the Croucher Foundation for support. A. C. C. Y. and T. M. gratefully acknowledge support from the Japan Society for the Promotion of Science.

[1] C. C. Yu and A. K. Petford-Long, J. Appl. Phys. **85**, 5753 (1999).
[2] R. Nakatani, K. Hoshino, S. Noguchi, and Y. Sugita, Jpn. J. Appl. Phys., Part 1 **33**, 133 (1994).
[3] K. Matsuda, A. Kamijo, T. Mitsuzuka, and H. Tsuge, J. Appl. Phys. **85**, 5261 (1999).
[4] P. Bayle-Guillemaud, A. K. Petford-Long, T. C. Anthony, and J. A. Brug, IEEE Trans. Magn. **32**, 4627 (1996).
[5] J. N. Chapman, J. Phys. D **17**, 623 (1984).
[6] J. C. S. Kools, Th. G. S. M. Rijks, A. E. M. De Veirman, and R. Coehoorn, IEEE Trans. Magn. **31**, 3918 (1995).
[7] L. Néel, Comptes Rendus **255**, 1676 (1962).
[8] X. Portier, A. K. Petford-Long, P. Bayle-Guillemaud, T. C. Anthony, and J. A. Brug, J. Magn. Magn. Mater. **198–199**, 110 (1999).
[9] A. K. Petford-Long, X. Portier, P. Bayle-Guillemaud, T. C. Anthony, and J. A. Brug, Microsc. Microanal. **4**, 325 (1998).
[10] L. J. Heyderman, J. N. Chapman, and S. S. P. Parkin, J. Phys. D **27**, 881 (1994).
[11] L. J. Heyderman, H. Niedoba, H. O. Gupta, and I. B. Puchalska, J. Magn. Magn. Mater. **96**, 125 (1991).
[12] R. Schäfer, A. Hubert, and S. S. P. Parkin, IEEE Trans. Magn. **29**, 2738 (1993).
[13] D. O. Smith and K. J. Harte, J. Appl. Phys. **33**, 1399 (1962).
[14] M. F. Gillies, J. N. Chapman, and J. C. S. Kools, J. Appl. Phys. **78**, 5554 (1995).